Low stoichiometry operation of the anode side of a low-temperature proton exchange membrane fuel cell – A modeling study

Liu, Wei; Berning, Torsten; Liso, Vincenzo

Published in:
International Journal of Hydrogen Energy

DOI (link to publication from Publisher):
10.1016/j.ijhydene.2023.06.288

Publication date:
2024

Document Version
Publisher's PDF, also known as Version of record

Available online at www.sciencedirect.com

ScienceDirect

journal homepage: www.elsevier.com/locate/he

Low stoichiometry operation of the anode side of a low-temperature proton exchange membrane fuel cell – A modeling study

W. Liu[*], *T. Berning*, *V. Liso*

Department of Energy Technology, Aalborg University, 9220 Aalborg, Denmark

HIGHLIGHTS

- An anode fuel cell CFD model includes the bipolar plate, channel, gas diffusion layer, microporous layer and catalyst layer.
- Demonstration that the anode side can be operated at a very low stoichiometry of 1.01.
- Demonstration that fuel cell anode can operate on completely dry inlet gases employing the water uptake layer.

ARTICLE INFO

Article history:
Received 23 December 2022
Received in revised form
24 May 2023
Accepted 25 June 2023
Available online 13 July 2023

Keywords:
PEMFC
Low stoichiometry operation
CFD
CFX

ABSTRACT

A single-channel proton exchange membrane fuel cell model (anode side) based on computational fluid dynamics is used to investigate the possibility of operating a fuel cell at low stoichiometric flow ratios using completely dry inlet hydrogen. A case study of three different stoichiometric flow ratios ($\xi = 1.01$, $\xi = 1.03$, $\xi = 1.05$), three different operating temperatures (343.15 K, 347.15 K, 353.15 K), and three different operating pressures (1 atm, 1.2 atm and 1.5 atm) are presented. It is found that the predicted hydrogen concentration and relative humidity (RH) in the catalyst layer (CL) have opposite trends: the RH in CL decreases with increasing stoichiometric flow ratios, but it reaches 100% at the outlet. While hydrogen concentration in CL increases with increasing stoichiometric flow ratios and the largest difference is at the inlet, with a maximum of 3.6%. The results also suggest that PEM fuel cells may be operated in a stoichiometric flow ratio as low as $\xi = 1.01$ at the anode side. This cell operation would allow open-ended anode operation without a recirculation system, thus significantly reducing system complexity and cost. The CFD code is disclosed to provide a starting point for more complex model development.

Introduction

Fuel cells are electrochemical devices that convert chemical energy into electricity. In the case of low-temperature proton exchange membrane (PEM) fuel cells, hydrogen is converted with oxygen from air to produce water and electricity with heat as the by-product. The electrochemical reactions that occur inside a PEMFC are:

Cathode: $O_2 + 4H^+ + 4e^- => 2H_2O$ (1)

* *Corresponding author.*
E-mail address: wli@et.aau.dk (W. Liu).

https://doi.org/10.1016/j.ijhydene.2023.06.288

Anode: $2H_2 => 4H^+ + 4e^-$ (2)

Combined: $O_2 + 2H_2 => 2H_2O$ (3)

Compared with batteries, the advantages are higher energy density, continuous power supply and convenience of refueling. Moreover, the fuel cell efficiency is usually higher than 60% [1].

As shown in Fig. 1, a single fuel cell typically consists of the membrane-electrode-assembly (MEA) in the center of the cell, where the membrane is typically Nafion, and the catalyst layer is coated to the membrane, forming a catalyst-coated membrane (CCM). The MEA is sandwiched between carbon fiber papers or woven cloth those serve as a gas "diffusion" layer (GDL), or more correctly: porous transport layer (PTL) [2], to transport the reactants gases to and the water away from the MEA, in addition to conducting electrons. The MEA with the adjacent GDL/PTL is then sandwiched between the bipolar plates (BPs) that contain the gas flow channels.

Owing to mass transport resistances, the reactant gases are to be supplied at an over-stoichiometry $\xi > 1$. The typical values for this over-stoichiometry are $\xi > 1.5$ at the cathode (air) side and $\xi > 1.2$ at the anode (hydrogen) side [3]. Therefore, hydrogen recirculation is necessary, which is the process of circulating the hydrogen gas within a fuel cell system to optimize its performance and efficiency.

Berning and Kær proposed low-stoichiometry fuel cell operation and suggested a definition of $\xi < 1.5$ at the cathode side and $\xi < 1.2$ at the anode side [3,4]. An alternative to hydrogen recirculation is the so-called "flow-shifting [5]", where the hydrogen alternatively switches direction between inlet and outlet, and only as much hydrogen is added to the gas stream as is consumed in the electrochemical reaction. Similar to the use of hydrogen recirculation, the problem here is the cross-over and accumulation of the nitrogen at the anode side, along with the build-up of water (vapor). Therefore, in both cases, flow shifting or the use of a recirculation pump, the anode side must be periodically purged, resulting in a hydrogen loss. It has also been observed that the movement of a nitrogen front in the fuel cell leads to catalyst degradation [6].

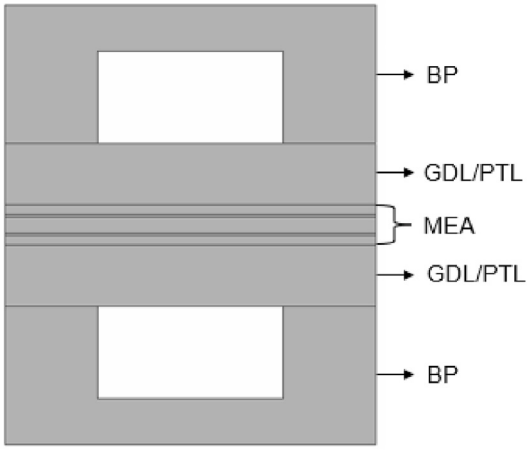

Fig. 1 – Single fuel cell geometry.

In general, the fuel cell gas supply and conditioning system are very complex [7–9], typically including a pump or ejector, humidifier, circulating gas path and so on. The ejector works by employing the shear force of the high-speed fluid to entrain the low-pressure fluid without electricity consumption [10]. In addition to being cost factors, these parasitic systems at both the cathode and anode sides can significantly reduce overall system efficiency and power density.

To increase the efficiency and power density of PEM fuel cell systems, as well as reduce the cost, it is desirable to operate the fuel cell at a low stoichiometric flow ratio. On the cathode side, our research group had done prior work, and the results suggested that operation at stoichiometric flow ratios as low as $\xi = 1.2$ at the cathode side appears feasible [3], provided that the so-called interdigitated flow field is employed that enhances mass transport of the oxygen to the catalyst layer.

While the vast number of PEM research focuses on the cathode side [11–14] because it is where the higher amount of Pt catalyst has to be used, a better fundamental understanding of the mass transfer at the anode side could be just as important. If it should be feasible to operate the fuel cell anode in "open anode [15–17]" mode at a very low stoichiometry, then the cost of not only the recirculation pump or ejector could be saved but also reducing system complexity and size. As the pump is also powered by the fuel cell (as high as 10% of the generated fuel cell stack power [4]), an increase in system efficiency can also be expected. Almost all previous studies have not lowered the stoichiometric flow ratio below 1.05. Therefore, this paper's subject is a fundamental understanding of the feasibility of operating a PEMFC at a reduced anode stoichiometric flow ratio as low as possible.

In this study, the hydrogen that enters the fuel cell is completely dry (0% RH) as it emerges from the high-pressure vessel. The previous results indicated that it might be possible to operate the fuel cell on completely dry reactant gases when a water uptake layer is employed [3,18], and it was successfully demonstrated by Monroe et al. [19] and Ge et al. [20] that they can work in principle.

Nine different cases are investigated: anode pressure of 1 atm, 1.2 atm and 1.5 atm; operating temperatures of 343.15 K (70 °C), 347.15 K (75 °C) and 353.15 K (80 °C), respectively. Additionally, there are three different stoichiometric flow ratios ($\xi = 1.01$, $\xi = 1.03$, $\xi = 1.05$) in every case. The focus is predominantly on the predicted hydrogen concentration and relative humidity (RH) in the catalyst layer (CL). The computational fluid dynamics (CFD) model is implemented as a standalone ANSYS CFX 2022 R1, which will be disclosed to the public, providing a starting point for more complex model development.

Model description

In this study, the steady-state multi-component model is isothermal and three-dimensional. The flow in the channels is assumed laminar. Diffusion is dominant in porous medium calculating by Fick's law. Moreover, Darcy's law is applied to express momentum loss.

Geometry

The geometry of the anode side employed for the simulations is shown in Fig. 2. The formulation allows us to calculate and investigate the effect of species concentration in three directions (X, Y, Z) due to the geometry. To reduce the size of the computational domain, we take advantage of the symmetry of the cell and hence decrease computational cost. Therefore, symmetry conditions are imposed on the geometry's left/right side.

The geometrical parameters are given in Table 1.

Computational mesh

Fig. 3 shows the computational mesh and multi-domain: domain I (bipolar plate), domain II (channel), domain III (gas diffusion layer), domain IV (micro-porous layer) and domain V (catalyst layer), used for this study. The five domains are all coupled through appropriate boundary exchange terms and an iterative solution procedure. Ensure that the number of layers in each domain is greater than or equal to 5. According to the structure of the fuel cell, two increasing grid numbers of 21,600 and 55,963 were used to check mesh independence. The results showed that the difference in the pressure at the outlet corresponding to 21,600 and 55,963 grid numbers is less than 0.42 Pa, which means the error is very small. In order to save the calculation time of numerical simulation, the number of meshes of 21,600 was selected to divide the geometric model. The cases presented here have all been calculated on a workstation with a 3.10 GHz and 20 cores. The number of iterations required to obtain converged solutions ranged from 4000 to 20,000; the latter required about 3 h of CPU time for each operating condition.

Model assumptions

A fuel cell model usually involves both microscale and macroscale geometric features and transport processes. To create a numerically tractable 3-D model, we adopt several simplifying assumptions.

Table 1 – Geometrical parameters.

	Value	Units
Channel width	0.6	mm
Channel height	0.3	mm
Channel length	200	mm
Land width	0.6	mm
GDL thickness	0.2	mm
MPL thickness	0.03	mm
CL thickness	0.01	mm

- the fuel cell operates under steady-state conditions;
- all gases are assumed to be ideal gases and pure gas;
- the flow in the channels is considered laminar;
- the cell is isothermal.
- hydrogen crossover is neglected.

Model equations

The steady-state equations of mass and momentum can be written as follows in a stationary frame:

The continuity equation:

$$\nabla\cdot(\rho u)=0 \tag{4}$$

And momentum equation:

$$\nabla\cdot(\rho u\otimes u-\mu\nabla u)=-\nabla\cdot\left(P+\frac{2}{3}\mu\nabla\cdot u\right)+\nabla\cdot\left(\mu(\nabla u)^{T}\right) \tag{5}$$

Where ρ is the gas density (kg/m^3), u is the velocity vector (m/s) $u=(u,v,w)$, P is the pressure (Pa) and T is the temperature (K). Darcy's law is commonly used for flows in the porous medium [21]. The permeability of the porous medium used is 18×10^{-12} m^2 [22].

The mass fraction is related to the molar fraction:

$$y_i=\frac{x_iM_i}{\sum x_iM_i} \tag{6}$$

where i donates different species (i.e. hydrogen and water vapor), M is the molecular weight ($M_{H_2}=2$ g/mol, $M_{H_2O}=$

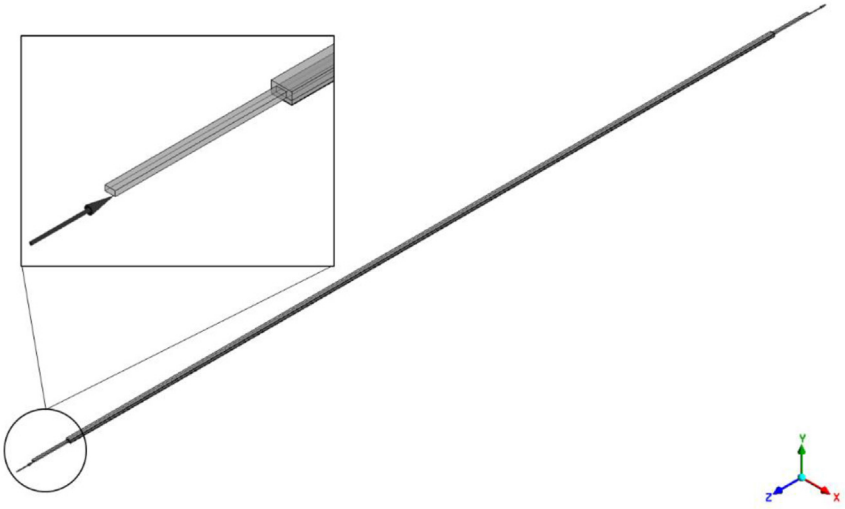

Fig. 2 – The geometry of the anode side in a single-channel fuel cell.

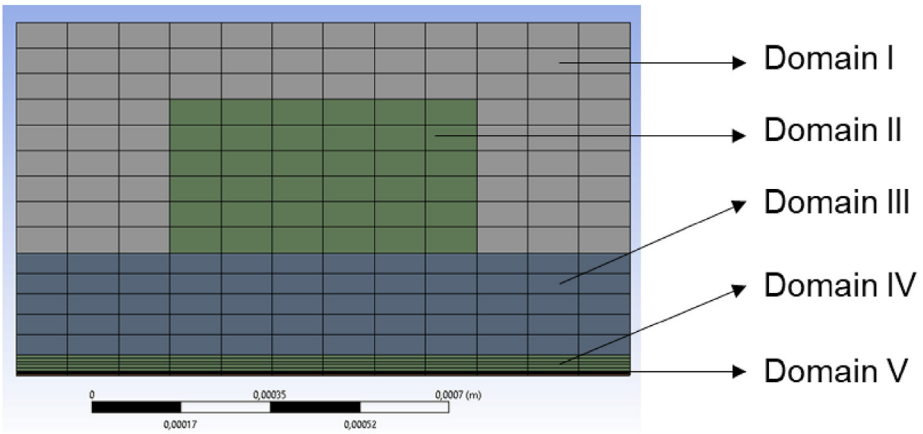

Fig. 3 – The computational mesh of a single-channel fuel cell.

Table 2 – Matrix of cases.

T P	1 atm	1.2 atm	1.5 atm
343.15 K	Case 1	Case 2	Case 3
348.15 K	Case 4	Case 5	Case 6
353.15 K	Case 7	Case 8	Case 9

18 g/mol). The sum of all mass fractions is equal to unity. The density is calculated by ideal gas assumption:

$$\rho = \frac{P_i M_i}{RT} \tag{7}$$

where R is the ideal gas constant, 8.314 J/mol/K.

Set mass flow rate for inlet boundary condition and mass fraction of hydrogen is set to 1.

The hydrogen mass flow rate (kg/s) at inlet is:

$$S_{H_2} = \xi \times I \times \frac{M_{H_2}}{(2F)} \tag{8}$$

where F is the Faraday constant (96,487 C/mol), and I is the current (A). M is the molecular weight of the specific species. ξ is the stoichiometric flow ratio.

The outlet boundary condition is static pressure, which is set to zero, and it depends on the reference pressure in this model.

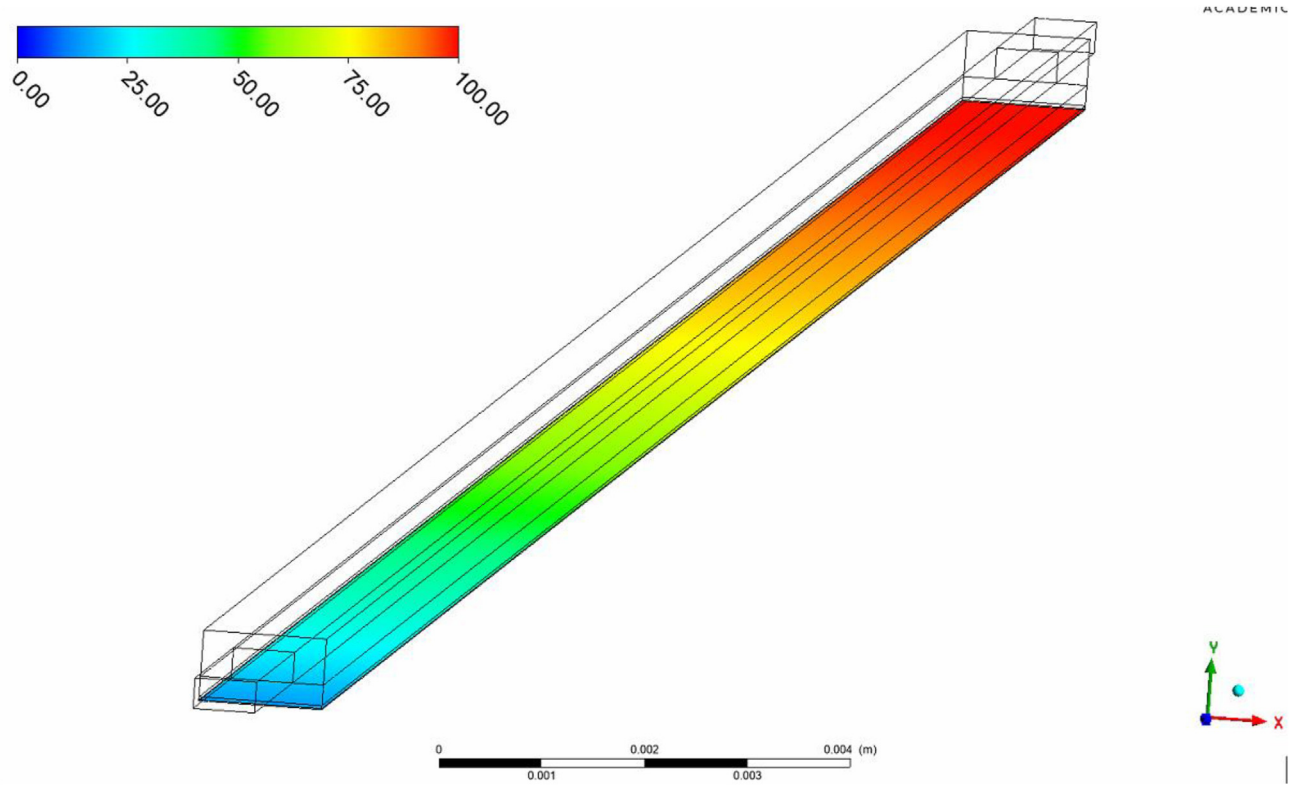

Fig. 4 – RH distribution in Case 1 (ξ = 1.01, 1 atm, 343.15 K).

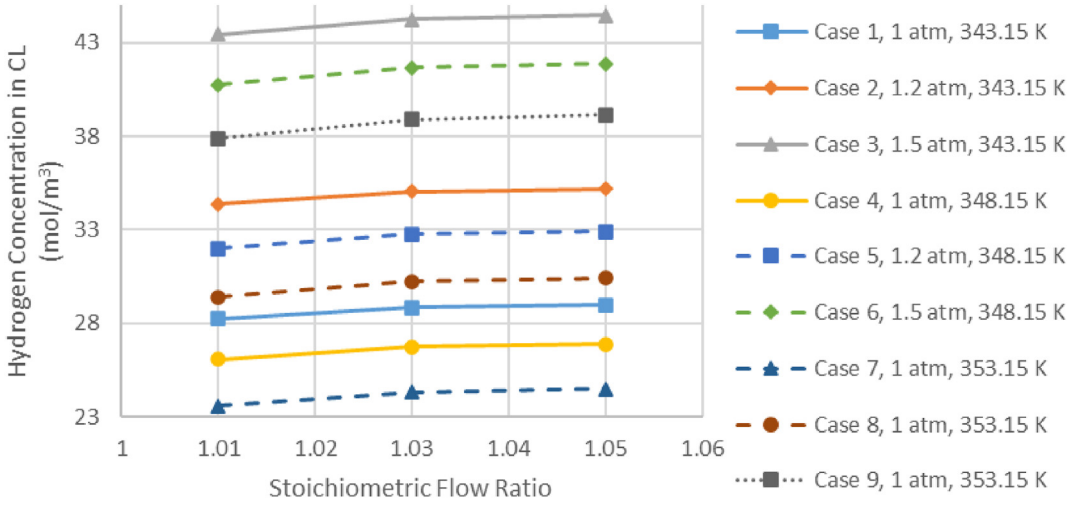

Fig. 5 – Calculated hydrogen concentration in CL for all cases investigated.

The saturation pressure of water vapor, P_{sat} (Pa), from the Antoine Equation [23] has been approximated by:

$$P_{sat} = 133.233 \times 10^{(8.07131 - 1730.63 / (233.426 + (T - 273.15)))} \quad (9)$$

here the T is in K.

The hydrogen sink term (kg/s) in the CL is defined according to the Faraday law as:

$$Sink_{H_2} = -I \times \frac{M_{H_2}}{(2F)} \quad (10)$$

The water source term (kg/s) in the CL (assuming the RH at the outlet is 100% and the water source term is uniform), is:

$$Source_{H_2O} = (\xi - 1) \times I \times P_{sat} \times \frac{M_{H_2O}}{2F \times P_{ref} \times \left(1 - \frac{P_{sat}}{P_{ref}}\right)} \quad (11)$$

where P_{ref} is the reference pressure, 1 atm.

The mass transport equation in the porous medium becomes:

$$\nabla \cdot (\rho u \varepsilon y) - \nabla \cdot (\rho D \varepsilon \nabla y) = S \quad (12)$$

Where ε is the porosity, D is the diffusivity (m^2/s).

For the binary diffusivities $D_{H_2O-H_2}$ [24] experimentally obtained were taken and scaled with the temperature and pressure according to:

$$D^{eff}_{H_2O-H_2} = D_{H_2O-H_2} \left(\frac{P_0}{P}\right) \left(\frac{T}{T_0}\right)^{1.5} \quad (13)$$

The binary diffusivities $D^{porous}_{H_2O-H_2}$ in porous media have been corrected for the porosity:

$$D^{\varepsilon}_{H_2O-H_2} = D^{eff}_{H_2O-H_2} (\varepsilon)^{1.5} \quad (15)$$

The porosities of GDL, MPL and CL are 0.88, 0.7 and 0.5, respectively.

Results and discussion

The goal of this study was to elucidate the feasibility of operating the PEM fuel cell at low stoichiometric flow ratios with pure hydrogen at the anode. The particularly important issue was the question of whether the fuel cell would be sufficiently

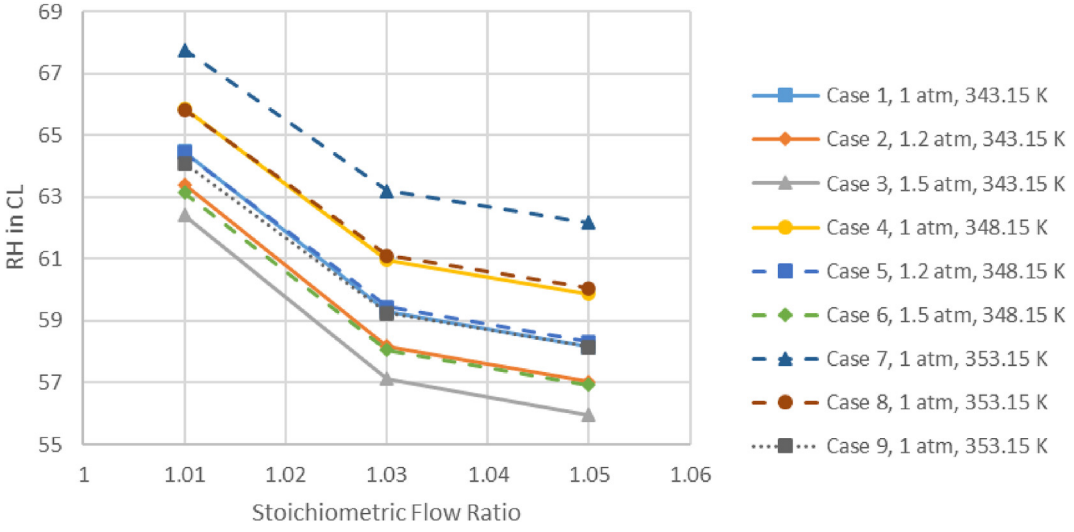

Fig. 6 – Calculated RH in CL for all cases investigated.

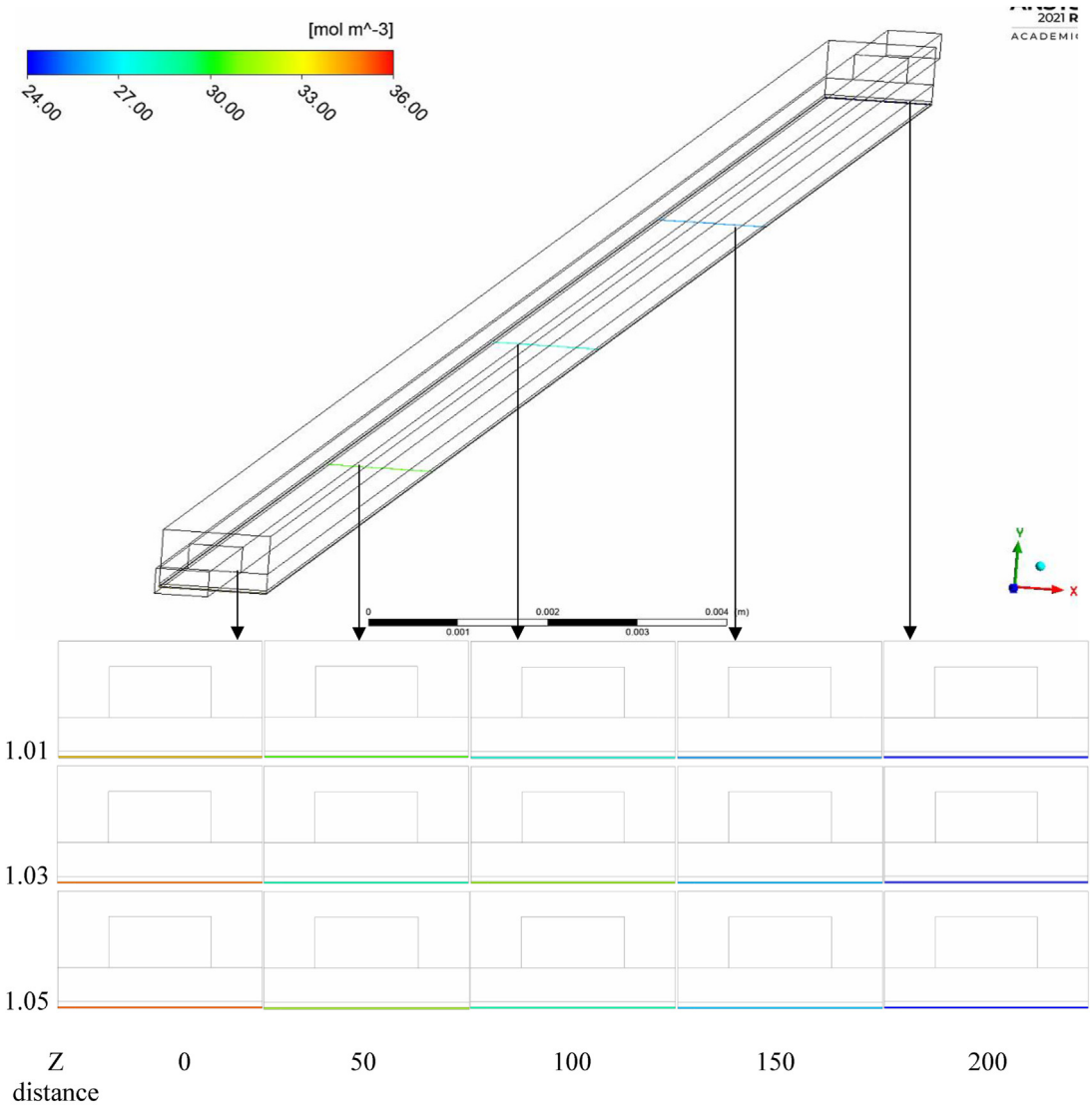

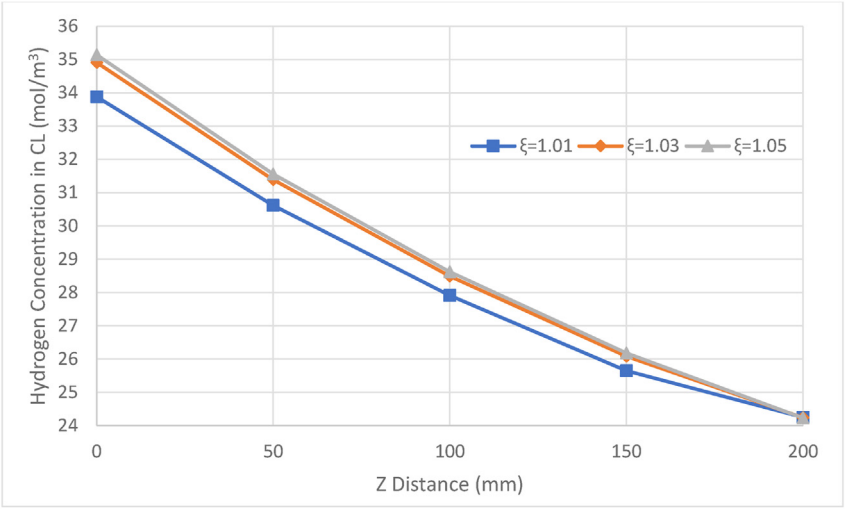

Fig. 7 – Predicted Hydrogen concentration for Case 1 at a current density of 0.6 A/cm^2 and $\xi = 1.01$, $\xi = 1.03$ and $\xi = 1.05$.

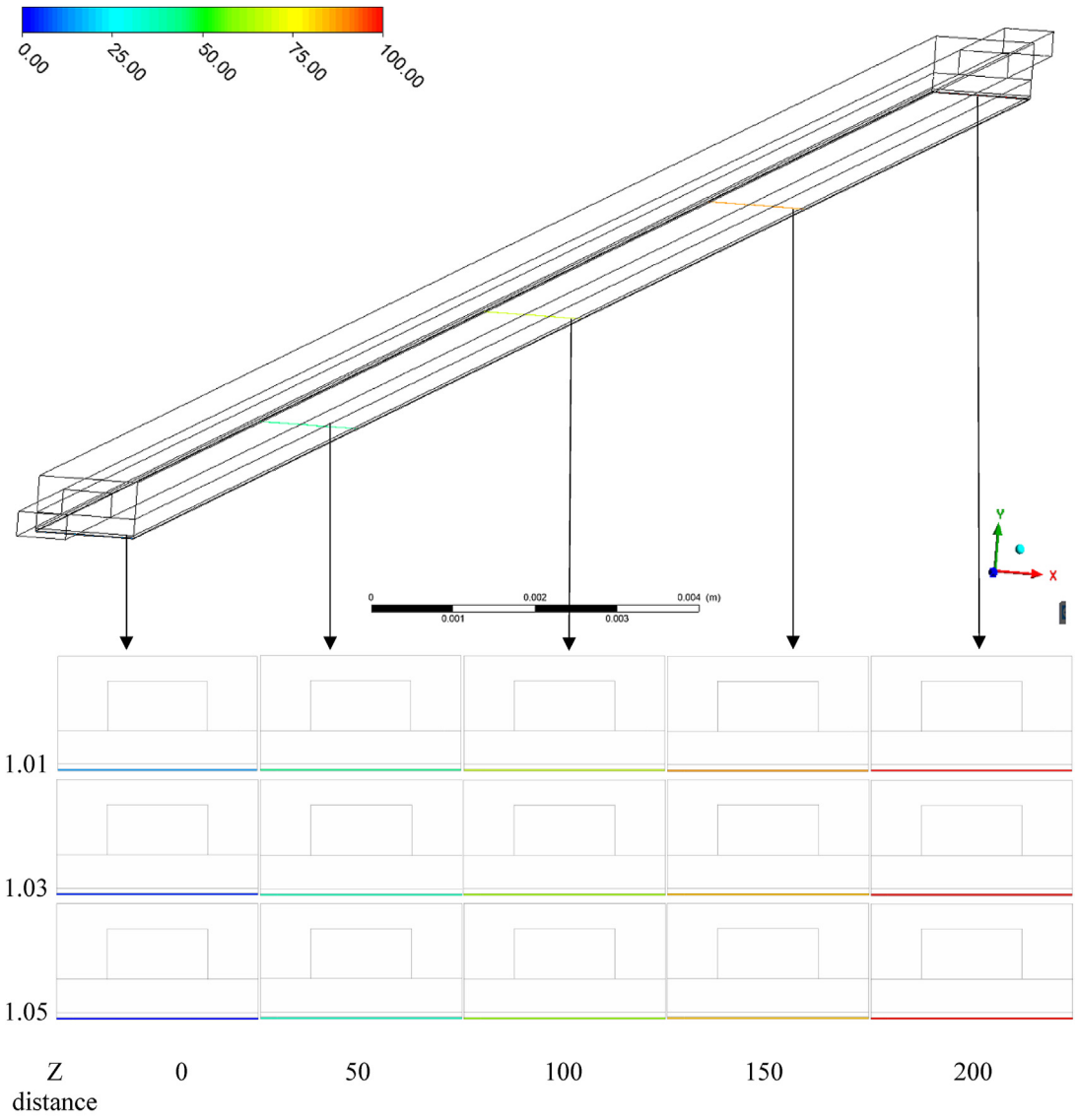

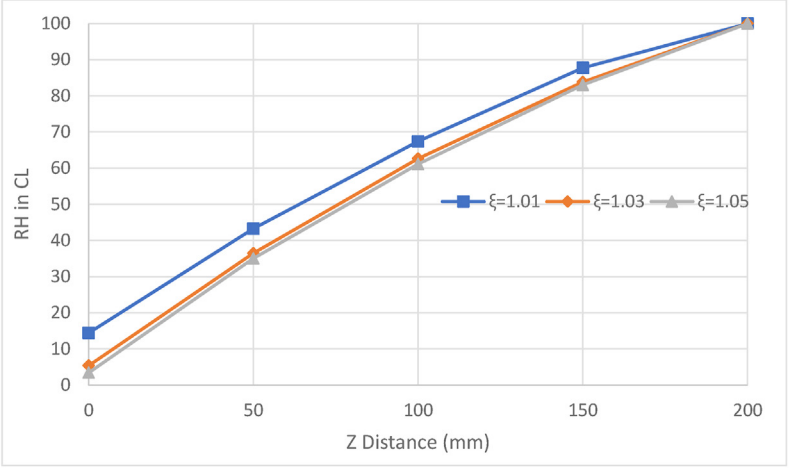

Fig. 8 – Predicted RH for Case 1 at a current density of 0.6 A/cm^2 and $\xi = 1.01$ $\xi = 1.03$ and $\xi = 1.05$.

humidified under the given operating conditions, especially when the stoichiometric flow ratio was under 1.05. The matrix of cases investigated is shown in Table 2. Usually, the frequent standard operating pressure in PEM fuel cell is greater than atmospheric pressure, and the operating temperature is between 50 °C and 90 °C [25,26].

In this study, it was decided to reduce the operating pressure from 1.5 atm to 1 atm and conduct the simulations for Case 1, Case 2 and Case 3. Then, the case was repeated with an increased operating temperature in Case 4-Case 9 from 343.15 K to 353.15 K. Moreover, there are three different stoichiometric flow ratios (1.01, 1.03, 1.05) in every case.

Comparison of all cases

The results for 9 cases will be compared in the following. One of the results on RH inside the catalyst layer is shown in Fig. 4. Obviously, it increases along the channel and the RH = 100% at the outlet. Note that the outlet here is the end of the fuel cell, not the actual gas outlet and the reason for this setup is to be closer to the actual situation and reduce the influence of external environment to improve accuracy. 100% RH proves the water source term and hydrogen sink term mentioned above are correct. Only the result for Case 1 is shown because the rest of the cases have almost same results.

The general finding in Fig. 5 is that increasing the stoichiometric flow ratio yields a higher hydrogen concentration in CL, but the change is slight. Moreover, this change with pressure also has the same trend when focusing on Case 1, Case 2 and Case 3. On the other hand, the hydrogen concentration is declining for elevated temperature cases.

Fig. 6 shows a comparison of the calculated RH in CL for all cases. An overall comparison can be made by looking at the calculated RH at the anode catalyst layer. The RH in CL decreases with increasing stoichiometric flow ratio, as the hydrogen partial pressure increases with increasing stoichiometric flow ratio clearly. Moreover, the temperature also has the same trend when focusing on Case 1, Case 4 and Case 7. On the other hand, the RH is declining for elevated pressure cases.

Reference case (Case 1)

Case 1 in this paper was conducted at an absolute cell pressure of 1 atm specified at the anode channel outlet, and an operating cell temperature of 343.15 K which was applied at the outer boundaries of the bipolar plate domains and for the incoming gas streams. The stoichiometric flow ratio was varied, starting from a value of 1.05 and decreasing toward 1.01. The incoming RH at the anode side was kept at zero. Next, some aspects of Case 1 will be analyzed exemplarily in detail with different stoichiometric flow ratios. Moreover, the simulation results/trends are consistent with the results [27–29].

Hydrogen concentration in CL

In the following section, detailed results will be presented for stoichiometric flow ratios of 1.01, 1.03 and 1.05, respectively. The results shown here are at a current density of 0.6 A/cm^2. Fig. 7 shows that the hydrogen concentration exhibits an almost one-dimensional distribution with the strongest variation being along the channel. Moreover, hydrogen concentration in CL increases with increasing stoichiometric flow ratios but slightly and the largest difference is at the inlet, with a maximum of 3.6%, and concentration tends to be the same at the outlet (24.24 mol/m^3).

RH in CL

Of central importance for the current study is the RH distribution inside the cell. Out of reasoning, in general, the RH should be lower when the stoichiometric flow ratio is increased. Fig. 8 shows the modeling result for the three different stoichiometric flow ratios. Like the previously shown hydrogen distribution, the RH distribution exhibits an almost one-dimensional behavior with only variations in the along-the-channel direction. For all cases, Fig. 8 shows the result that the fuel cell becomes fully humidified (RH = 100%) at the outlet despite the entirely dry inlet gas streams and the stoichiometric flow ratio is a little bit higher than 1.

Conclusion

A modeling study has been presented to elucidate appropriate operating conditions to run a fuel cell at a low stoichiometric flow ratio in order to simplify the fuel cell system. Based on the previous work, we focused on the feasibility of reducing the stoichiometric flow ratio ($\xi < 1.05$) at the anode side in this paper. The following conclusions can be drawn:

(1) In all investigated cases, hydrogen concentration and RH have opposite correlations with respect to the stoichiometric flow ratios. That is, the RH in CL decreased with increasing stoichiometric flow ratios, while hydrogen concentration in CL increased with increasing stoichiometric flow ratios.
(2) The results were obtained for a stoichiometric flow ratio as low as $\xi = 1.01$ at the anode inlet. This means that PEM fuel cells may be operated in a steady-state mode without a recirculation system, which would simplify the system complexity and reduce the cost. The complete fuel cell model with membrane will be built to verify cell performance and enable more precise water management in future work.
(3) In all cases, appropriate CFD modeling can lead to design of experiments.

With this free open CFD implementation of a PEMFC model (shared on GitHub), anyone with access to the ANSYS CFX installation can readily run or extend a simulation, substitute material parameterizations, add new model features or conduct parameter studies.

Declaration of competing interest

The authors declare that they have no known competing financial interests or personal relationships that could have appeared to influence the work reported in this paper.

Acknowledgments

Wei Liu appreciates China Scholarship Council (CSC) for the financial support.

REFERENCES

[1] O'Hayre R, Cha SW, Colella W, et al. Fuel cell fundamentals [M]. John Wiley & Sons; 2016.
[2] Li Qingyu, et al. Numerical study on oxygen transport pattern in porous transport layer of proton exchange membrane electrolysis cells. eTransportation 2023;15:100210.
[3] Berning T. Low stoichiometry operation of a proton exchange membrane fuel cell employing the interdigitated flow field—A modeling study[J]. Int J Hydrogen Energy 2012;37(10):8477–89.
[4] Berning T, Odgaard M, Kær SK. Low stoichiometry operation of a polymer electrolyte membrane fuel cell employing the interdigitated flow field design[J]. ECS Trans 2011;41(1):1897.
[5] Lienkamp S, Willimowski P, Arthur DA. Control of nitrogen fraction in a flow shifting fuel cell system. U.S. Patent 2011;7:862–948. 1-4.
[6] Chen D, Pei P, Ren P, et al. Analytical methods for the effect of anode nitrogen concentration on performance and voltage consistency of proton exchange membrane fuel cell stack[J]. Energy 2022;258:124850.
[7] Dadvar M. Analysis of design parameters in anodic recirculation system based on ejector technology for PEM fuel cells: a new approach in designing[J]. Int J Hydrogen Energy 2014;39(23):12061–73.
[8] Yin Yan, et al. Numerical investigation of an ejector for anode recirculation in proton exchange membrane fuel cell system. Energy Convers Manag 2016;126:1106–17.
[9] Besagni Giorgio, et al. Application of an integrated lumped parameter-CFD approach to evaluate the ejector-driven anode recirculation in a PEM fuel cell system. Appl Therm Eng 2017;121:628–51.
[10] Han J, Feng J, Chen P, et al. A review of key components of hydrogen recirculation subsystem for fuel cell vehicles[J]. Energy Conversion and Management: X; 2022, 100265.
[11] Qu S, Li X, Hou M, et al. The effect of air stoichiometry change on the dynamic behavior of a proton exchange membrane fuel cell[J]. J Power Sources 2008;185(1):302–10.
[12] Chen H, Liu B, Liu R, et al. Optimal interval of air stoichiometry under different operating parameters and electrical load conditions of proton exchange membrane fuel cell[J]. Energy Convers Manag 2020;205:112398.
[13] Liu D, Lin R, Feng B, et al. Investigation of the effect of cathode stoichiometry of proton exchange membrane fuel cell using localized electrochemical impedance spectroscopy based on print circuit board[J]. Int J Hydrogen Energy 2019;44(14):7564–73.
[14] Wang X, Chen J, Quan S, et al. Hierarchical model predictive control via deep learning vehicle speed predictions for oxygen stoichiometry regulation of fuel cells[J]. Appl Energy 2020;276:115460.
[15] Kurnia JC, Sasmito AP, Shamim T. Advances in proton exchange membrane fuel cell with dead-end anode operation: a review[J]. Appl Energy 2019;252:113416.
[16] Chen B, Wang J, Yang T, et al. Mitigation studies of carbon corrosion by optimizing the opening size of the cathode outlet in a proton exchange membrane fuel cell with dead-ended anode[J]. Energy Convers Manag 2016;119:60–6.
[17] Hosseini M, Afrouzi HH, Arasteh H, et al. Energy analysis of a proton exchange membrane fuel cell (PEMFC) with an open-ended anode using agglomerate model: a CFD study[J]. Energy 2019;188:116090.
[18] Berning T. On water transport in polymer electrolyte membranes during the passage of current[J]. Int J Hydrogen Energy 2011;36(15):9341–4.
[19] Monroe CW, Romero T, Mérida W, et al. A vaporization-exchange model for water sorption and flux in Nafion[J]. J Membr Sci 2008;324(1–2):1–6.
[20] Ge S, Li X, Yi B, et al. Absorption, desorption, and transport of water in polymer electrolyte membranes for fuel cells[J]. J Electrochem Soc 2005;152(6):A1149.
[21] Berning T, Lu DM, Djilali N. Three-dimensional computational analysis of transport phenomena in a PEM fuel cell[J]. J Power Sources 2002;106(1–2):284–94.
[22] Gostick JT, Fowler MW, Ioannidis MA, et al. Capillary pressure and hydrophilic porosity in gas diffusion layers for polymer electrolyte fuel cells[J]. J Power Sources 2006;156(2):375–87.
[23] Thomson GW. The Antoine equation for vapor-pressure data [J]. Chem Rev 1946;38(1):1–39.
[24] Cussler EL. Diffusion: mass transfer in fluid systems[M]. Cambridge university press; 2009.
[25] Liso V, Araya SS, Olesen AC, et al. Modeling and experimental validation of water mass balance in a PEM fuel cell stack[J]. Int J Hydrogen Energy 2016;41(4):3079–92.
[26] Berning T, Djilali N. Three-dimensional computational analysis of transport phenomena in a PEM fuel cell—a parametric study[J]. J Power Sources 2003;124(2):440–52.
[27] Liu D, Lin R, Feng B, et al. Investigation of the effect of cathode stoichiometry of proton exchange membrane fuel cell using localized electrochemical impedance spectroscopy based on print circuit board[J]. Int J Hydrogen Energy 2019;44(14):7564–73.
[28] Berning T, Djilali N. Three-dimensional computational analysis of transport phenomena in a PEM fuel cell—a parametric study[J]. J Power Sources 2003;124(2):440–52.
[29] Mert SO, Dincer I, Ozcelik Z. Performance investigation of a transportation PEM fuel cell system[J]. Int J Hydrogen Energy 2012;37(1):623–33.